UNIVERSITY OF ILLINOIS

May 9 1989

THIS IS TO CERTIFY THAT THE THESIS PREPARED UNDER MY SUPERVISION BY

Julie Peshkin

ENTITLED The Study of Intermolecular Interactions of

Carbazole in Supercritical Fluids Carbon Dioxide and Fluoroform

IS APPROVED BY ME AS FULFILLING THIS PART OF THE REQUIREMENTS FOR THE

DEGREE OF Bachelor of Science

Charles A. Eckert

Instructor in Charge

APPROVED: R.C. Alkire

HEAD OF DEPARTMENT OF Ciemical Engineering

O-1364

The Study of Intermolecular Interactions of Carbazole in Supercritical Fluids Carbon Dioxide and Fluoroform

By

Julie Peshkin

Thesis

for the
Degree of Bachelor of Science
i
Chemical Engineering

College of Liberal Arts and Sciences
University of Illinois
Urbana, Illinois

1989

TABLE OF CONTENTS

LIST OF TABLES

LIST OF FIGURES

SUMMARY

Supercritical fluids possess a unique combination of qualities which make them extremely valuable for extraction and separation processes. This research uses absorption and fluorescence spectroscopy to examine the frequency shifts of dilute carbazole solutions in SCF CO_2 and CHF_3. The results of this work indicate that wavelength shifts are a function of solution density (i.e., pressure), that they are highly sensitive to density changes near the critical region, and that these effects are somewhat more pronounced in polar solvents. The information from this work will be used in helping to design equations of state models to aid in the design of separation processes.

INTRODUCTION

A supercritical fluid (SCF) is one that has been heated and compressed above its critical temperature and pressure. In the SC region a fluid possesses properties of both a liquid and a gas in a combination which gives it a unique character. Specifically, a SCF has the density and solvent properties of a liquid and the transport properties and compressibility of a gas. In addition, small changes in temperature and pressure produce significant changes in the aforementioned properties. This unique combination makes SCF an effective solvent for many separation processes.

The goal of this research is to use fluorescence and absorption spectroscopy to study frequency shifts of dilute carbazole ($C_{12}H_9N$) solutions in SCF carbon dioxide (CO_2) and fluoroform (CHF_3). Experimental data will be used to observe how wavelength shifts vary with solvent, solute concentration, and proximity to the critical point. Ultimately, this data will be used with Lippert's equation (see Appendix) to examine the change in cavity size of the solute molecule as a function of proximity to the critical point of the solvent.

This research is valuable in helping us to understand the physical interactions occurring in SCF. The information can be used for the development of equations of state which will aid in the design of effective separation processes using SCF.

SURVEY OF LITERATURE

The supercritical region of a pure component is defined as the region above its critical temperature and pressure (Figure 1). In this area, the compound is strictly neither a gas nor a liquid, but it possesses properties of both which make it particularly interesting and valuable for extraction and separation processes. High density gives the SCF a high capacity for solute, high diffusivity and low viscosity lend the SCF gas-like mass transfer properties, and high compressibility makes the SCF extremely selective for solutes (i.e., small pressure changes lead to large density changes which implies large solubility changes) (Brennecke, 1984). In short, SCF offer the solvent properties of a liquid and the mass transfer properties of a gas.

Although SCF phenomena were observed over 100 years ago, it wasn't until the last 30 to 40 years that much research has been undertaken or applied to industry. In their review paper, Paulaitis and coworkers indicate the following as motivation for current interest in SCF technology:

1. Increasing energy costs for traditional extraction processes.
2. Stricter government regulations of solvents used for extractions.
3. More stringent pollution control.

(Paulaitis, et al, 1982)

Among the more comprehensive reviews of SCF extractions are those of Paulaitis and coworkers, Brennecke and Eckert, and McHugh and Krukonis.

Brennecke and Eckert suggest that supercritical fluid extraction (SCFE) is not acceptable for all separations, but that it can be useful for difficult ones. Due to high

capital costs and the potential hazards of working with high pressures and flammable solvents, they recommend using SCFE only when conventional methods provide inadequate solutions to separation or extraction difficulties. (Brennecke and Eckert, 1989). Applications for SCFE include separations of chemicals from water streams, decaffienation of coffee and tea, extraction of oil from seeds and food, fractionation of low vapor pressure oils, extraction of solvents, monomers, and oligomers, and fractionation of polymers, and regeneration of activated carbon (Paulaitis, et al, 1982).

In order to design these separation processes, it is necessary to have an equation of state (EOS) to model the phase behavior of the system. Existing EOS inadequately represent the behavior in the near-critical region and are thus ineffective for designing separation processes (Hess, 1987). Fluorescence and absorption spectroscopy are useful for gaining an understanding of molecular interactions in solution: information which is necessary for designing more accurate EOS.

At room temperature, most molecules are found in their lowest energy state--the ground state. Absorption occurs when molecules absorb a photon of energy and are promoted to higher energy or excited states. From the excited state, a molecule can undergo one of several processes illustrated in Figure 2. One option is for the molecule to fall from the excited vibrational state to the lowest energy vibrational state. This process occurs without the emission of radiation and is called internal conversion. The molecule can then return to the ground electronic state with the loss of a photon of energy, a process known as fluorescence (Skoog, 1985).

Due to internal conversion, fluorescence spectra occur at longer wavelengths than absorption spectra. According to Skoog, excitation at λ_1 or λ_2 will produce fluorescence at λ_3 (where $\lambda_1 > \lambda_2$ or λ_3). Internal conversion to the S_1 vibrational level

occurs quickly and is followed by loss of a photon of energy and return to an excited vibrational level of S_0. Because the spacing of these levels is similar, the fluorescence spectra are generally the mirror image of the absorption spectra (Lumb, 1978).

Frequency shifts result from solvent rearrangement around the excited state molecule (Figure 3). The lifetime of the excited state is long enough to allow for rearrangement. When the molecule emits a photon it falls to an unstable ground state which is at a higher energy level than the original stable configuration (Parker, 1968). The result is emission of energy at longer wavelengths than absorption. This phenomena is explained in detail by Ooshika (1954).

The Lippert equation is a commonly used expression for the frequency shift. In this equation, frequency shift is primarily a function of the solvent refractive index, the dielectric constant, and the size of the cavity around the chromophore in which the fluorophore resides.

Fluorescence is particularly favorable for large aromatic molecules and is sensitive enough to be used for examining extremely dilute solutions. These attributes make it particularly attractive for this research.

APPARATUS

The spectrometer assembly used for this experiment is pictured in Figure 4. The light source is a 1000W Xenon arc lamp powered by a Kratos 2PS 255 HR in a Kratos LH 151 universal lamp housing. Both the emission and the excitation monochromators are Kratos model GM252 with 252-30 gratings blazed at 300 nm and Kratos GMA Quartz push-pull adjustable lenses. Custom-built aluminum connectors enclose the optical path between the monochromators and the optical cell. The primary condensing lense for the monochromator is a 2.25 in. diameter f/1.15 and the condensing lens on the inlet to the optical cell is a Kratos model LHA 150/2 with a 6 in. focal length. The excitation monochromator also is equipped with a Kratos GMA 2560 predispersion prism. The photomultiplier tube is a Hamamatsu IP-28 in a Kratos D500 housing and it is powered by a Keithly model 247 high voltage source at -950 V. The stepper motor on the emission monochromator (for fluorescence) or the excitation monochromator (for absorbance) is computer controlled and coordinated with computer data acquisition of an intensity signal from a Keithly model 414A picoammeter.

The high pressure assembly used to introduce the sample into the optical cell is shown in Figure 5. The gas is introduced to the solvent and mixing vessels with a Haskel AG-151 air-driven compressor. The vessels are 3 in. ID, 0.25 in. thick 316SS pipe (approximate volume: 2000ml) sealed with a single 2-240 nitrile O-ring. The mixing vessel pressure is measured with a 15000 psi Heise gauge accurate to ±15 psi. Both vessels can be connected to a vacuum pump which uses a Varian model- thermocouple gauge to measure vacuum. Thermal mixing of the sample solution is

achieved by taping a variac-controlled heating tape to the side of the mixing vessel. All tubing in the system is 1/8" diameter 316SS High Pressure Equipment and the valves and connectors are HPE taper seals.

The optical cell was custom-designed and built in the machine shop. The windows are 1/2" diameter, 1/4" thick fused quartz (type T12 Optosil 1 from Heraeus Amersil, Inc.). The O-rings are viton sizes 2-012, 2-014, and 2.018. Brass O-rings are also used as back-up rings and to provide a physical barrier in front of the viton rings. Pressure in the optical cell is measured with a Texas Instruments model 140 quartz gauge accurate to ±3 psi. Temperature in the cell is controlled by a custom-built precision controller accurate to ±0.02°C. The temperature is measured by the resistance of an Omega type 44032 thermistor with a Keithly model 190 digital multimeter. The thermistor was calibrated against a National Bureau of Standards mercury thermometer. The optical cell is heated using four Melcor model CP1.4-71-06L peltier coolers attached to the bottom of the cell and powered by a low frequency/high current power supply designed and built in the electronics shop.

Detailed drawings of the pressure vessels and optical cell can be found in the appendix (Figures 6 and 7).

PROCEDURE

The sample solution is prepared by dissolving 0.1188g of carbazole in 10 ml methylene chloride in a septum bottle. The sample is prepared by placing 0.06 or 0.006 ml (for 10^{-6} and 10^{-7} mole fraction solutions) onto a piece of filter paper (predried in a vacuum oven) using a 100 microliter syringe. The carbazole used is from Aldrich Chemicals and is purified by recrystalization in acetone.

The sample-coated filter paper is hung in the mixing vessel and the vessel is sealed. A vacuum is then pulled on the vessel for about 5 minutes or until the gauge reads approximately 2 millitorr. The vessel is then flushed 3 times with about 100 psi of solvent. After this, the vessel is filled to 2200 to 2600 psi. At this time, temperature and pressure are recorded, the heating tape is turned on and allowed to heat to approximately 35°C, and the vessel is left for a minimum of 12 hours to allow for complete mixing. Before starting the experiment, two additional readings of temperature and pressure are taken so the exact composition in the mixing vessel can be determined.

The solvent vessel is prepared the same way as the mixing vessel (without addition of solute) and is filled with 1500-2000 psi of solvent.

The optical cell is flushed with several hundred pounds of solvent before use. It is then filled with 2000 psi of solvent and the temperature controller is turned on to allow ample time for the temperature to equilibrate. The sample solution is bled through the cell with approximately equal inlet and outlet flow rates at the desired pressure. Enough sample is bled through the cell to completely displace the solute.

This is confirmed by repeatedly observing the same intensity (on the picoammeter) of a major peak.

The sample is left in the optical cell for 10 minutes to allow the temperature to equilibrate. After four minutes, the power for the lamp is turned on and a minute later the lamp is turned on. Five minutes of illumination is considered sufficient for the fluorescence to come to steady state (Brennecke, 1984). For fluorescence experiments, the excitation wavelength is 308 nm and the sample is scanned from 320 to 520 nm. For absorption, the excitation wavelength scanned is 265 to 465 nm. In the remaining five minutes, the computer is set up for data acquisition. At the beginning and end of each scan, measurements of the optical cell temperature and pressure are recorded.

Ten scans are taken for each sample at approximately 100 psi increments (with smaller increments at pressures closer to the critical pressure). For subsequent runs, 50 to 100 psi of sample are bled through the optical cell and the procedure is repeated.

The CO_2 used is anaerobic grade from the Linde Division of Union Carbide. The fluoroform used is Dupont Freon 23 with two Alltech oxy-traps attached to reduce the oxygen concentration to less than 5 ppm.

RESULTS

Fluorescence and absorption spectra were taken for carbazole solutions of 10^{-6} and 10^{-7} mole fraction in both CO_2 and CHF_3. These runs were performed at 30 and 50°C for CHF_3 and 35 and 50°C for CO_2 and at pressures ranging from 750 to 2058 psia. A complete list of the experiments run and the critical properties of the solvent can be found in Tables 1 and 2. Table 3 is a detailed list containing each run and the temperature, pressure, and density of solution, and the wavelength of the major peak. Density and wavelengths were extracted from the raw data by a BASIC program which will not be included in this work.

Absorption spectra of carbazole in CO_2 show the major peak appearing at approximately 284 to 288 nm for densities ranging from 0.005 to 0.018 moles/cc (Figure 8). The spectra for carbazole in CHF_3 show the major peak at 284.5 to 285.5 nm corresponding to densities of 0.008 to 0.014 moles/cc (Figure 9). These trends are consistent with our expectations. Research by Kim and Johnston suggests that at higher densities the increased stabilization of the excitation state of the molecule lowers the transition energy (defined as $E_T = hc/\lambda_{max}$) and the major peak shifts to longer wavelengths (1987). However, they maintain that this effect should be more pronounced in polar solvents because changes in density result in more extreme changes in the dielectric constant. The dipole moment of CO_2 and CHF_3 can be found in the Appendix. Parker also examined solutions in polar solvents and notes that solvent interactions with both the ground and excited states is increased: "the corresponding decrease in energy of the excited state is slightly greater than that of the

ground state, and hence the absorption band shifts slightly toward the red," (1968) i.e., longer wavelengths. The inconsistency between the expected trends and the experimental results may indicate the significance of other effects such as the increased importance of quadrupole moments of CO_2 in the near critical region. The data also indicates that absorption is relatively independent of temperature yet is highly sensitive to pressure (density) changes, particularly in the near-critical region.

A comparison of wavelength and density for solutions of 10^{-6} and 10^{-7} mole fraction (Figures 10 and 11) suggests that wavelength is independent of solution concentration for both absorption and fluorescence spectra. This is what is expected at these dilute concentrations.

Fluorescence spectra were taken under the same conditions as the absorption spectra mentioned above. For these runs, the major peaks occurred at 329 to 332 nm for CO_2 and 328 to 331 nm for CHF_3 corresponding to densities of 0.005 to 0.018 and 0.003 to 0.015 moles/cc respectively (Figures 12 and 13). As with the absorption spectra, the trends found in this data are compatible with the expected results. The same arguments apply for the fluorescence data, and, again our expectations of higher wavelength shifts in the more polar solvent are not born out by the experimental data.

The wavelength shift of the major peak ($\nu_a - \nu_f$) for solutions of 10^{-6} mole fraction in both CO_2 and CHF_3 is compared in Figure 14. The shift in fluoroform is slightly greater than that in CO_2. Using Lippert's equation, it can be reasoned that wavelength shift may be due to one or more of the following effects: change in the solvent refractive index, α, the dielectric constant, ε, or the radius of the cavity where the fluorophore resides, a. The complexity of determining α and ε make analysis using Lippert's equation beyond the scope of this work, however, measurements of

wavelength shift are useful for future work in this area.

CONCLUSIONS

Based on the examination of dilute carbazole solutions in SCF carbon dioxide and fluoroform, the following conclusions can be made:

1. At higher solution densities, the wavelength of the major peak shifts toward red, or longer, wavelengths.

2. Wavelength shifts are relatively independent of temperature and solution concentration (at least for very dilute solutions).

3. Wavelength shifts are highly sensitive to pressure/density changes, particularly in the near critical region.

4. Wavelength shifts between fluorescence and absorption spectra are slightly more pronounced in polar solvents.

RECOMMENDATIONS

For future research, it is suggested that solutes with larger dipole moments be used. This will result in spectra with larger wavelength shifts which should, in turn, provide more conclusive results than this research.

It is also recommended that the information from this research be analyzed with respect to changes in the solvent refractive index and the dielectric constant. Lippert's equation could then be used (along with $\Delta\nu$ information) to determine if α and ϵ are changing or if the cavity size, a, is changing with proximity to the critical point.

REFERENCES

Brennecke, Joan F. "Fluorescence Spectroscopy Study of Dilute Pyrene Solutions in Supercritical Carbon Dioxide," diss., University of Illinois, 1984.

Brennecke, Joan F. and C. A. Eckert. "Phase Equilibria For Supercritical Fluid Process Design," Submitted to AIChE J. 2/89.

Hess, Barry S. "Supercritical Fluids: Measurement and Correlation Studies of Model Coal Compound Solubility and the Modeling of Solid-Liquid-Fluid Equilibria," diss., University of Illinois, 1987.

Kim, S. and K. P. Johnston. "Molecular Interactions in Dilute Supercritical Fluid Solutions," Ind. Eng. Chem. Res. 26(1987): 1206-1213.

Lakowicz, J. R. Principles of Fluorescence Spectroscopy. New York: Plenum, 1983.

Lumb, M.D. Luminescence Spectroscopy. New York: Academic, 1978.

McHugh, M. A., and V. J. Krukonis, Supercritical Fluid Extraction: Principles and Practice. Boston: Butterworths, 1986.

Ooshika, Y. "Absorption Spectra of Dyes in Solution," J. Physical Soc. Japan 9(1954): 594-602.

Parker, C.A. Photoluminescence of Solutions. Amsterdam: Elsevier, 1968.

Paulaitis, M. E., V. J. Krukonis, R. T. Kurnik, and R. C. Reid. "Supercritical Fluid Extraction," Rev. Chem. Eng. 1(1982): 179-250.

Skoog, Douglas A. Principles of Instrumental Analysis. 3rd ed. New York: Saunders, 1985.

ACKNOWLEDGEMENTS

I wish to thank Dr. Charles Eckert, my thesis advisor, for giving me the opportunity to work for him and for enthusiastically supporting my work in his group. I would also like to thank doctoral student Joan Brennecke for her guidance and support for my research and for always being available as a friend. Finally, I would like to thank my parents, Maryann and Buddy, whose love and support made this all possible.

APPENDIX

LIPPERT'S EQUATION

$$\bar{\nu}_a - \bar{\nu}_f = \frac{2}{hc}\left(\frac{\varepsilon-1}{2\varepsilon+1} - \frac{\eta^2-1}{2\eta^2+1}\right)\left(\frac{\mu^*-\mu}{a^3}\right)^2 + \text{constant}$$

η = solvent refractive index
ε = dielectric constant
h = Planck's constant
c = the speed of light
a = radius of the cavity in which the fluorophore resides
μ = ground state dipole moment
μ^* = excited state dipole moment

TABLE 1

Experiments Performed

Spectra	Solvent	Conc. (mol frac)	Temp (°C)	Run Number
Fluorescence	CO_2	$1.0x10^{-6}$	35	555-564
	CO_2	$1.0x10^{-6}$	50	565-575
	CO_2	$1.0x10^{-7}$	35	586-594
	CO_2	$1.0x10^{-7}$	50	576-585
	CHF_3	$1.0x10^{-6}$	30	657-666
	CHF_3	$1.0x10^{-6}$	50	637-646
	CHF_3	$1.0x10^{-7}$	30	647-656
	CHF_3	$1.0x10^{-7}$	50	627-636
Absorbance	CO_2	$1.0x10^{-6}$	35	598-606
	CO_2	$1.0x10^{-6}$	50	607-616
	CO_2	$1.0x10^{-7}$	50	617-626
	CHF_3	$1.0x10^{-6}$	30	667-676
	CHF_3	$1.0x10^{-6}$	50	677-686

TABLE 2

Supercritical Fluid Solvents

Solvent	T_c (K)	P_c (bars)	Dipole Moment (D)
Carbon dioxide	304.2	73.8	0
Fluoroform	299.0	48.2	1.65

TABLE 3

Experimental Data

Run #	T (°C)	P (psia)	ρ (gmol/cc)	ν (nm)
555	35.0	1876	0.017850	332.1
556	35.0	1974	0.018096	331.8
557	35.0	1738	0.017442	332.0
558	35.0	1534	0.016654	332.1
559	35.1	1368	0.015611	331.1
560	35.1	1293	0.014859	331.5
561	35.2	1200	0.012709	331.7
562	35.2	1173	0.010865	331.7
563	35.1	1134	0.007730	330.2
564	35.2	1102	0.006340	329.8
565	49.9	1976	0.015052	331.4
566	50.3	1873	0.014323	331.7
567	50.3	1705	0.012847	331.3
568	50.2	1543	0.010493	330.5
569	49.8	1389	0.007755	330.7
571	49.8	1288	0.006307	330.7
572	49.8	1205	0.005409	329.7
573	49.8	1171	0.005094	328.5
574	49.8	1141	0.004837	329.0
575	49.9	1097	0.004484	328.5
576	50.2	1911	0.014600	331.2
577	50.1	1866	0.014332	331.4
578	50.1	1650	0.012252	330.6
579	50.1	1536	0.010409	330.7
580	50.1	1364	0.007279	---
581	50.2	1258	0.005905	329.2
582	50.3	1186	0.005184	329.8
583	50.2	1158	0.004948	329.2
584	50.3	1127	0.004688	329.4
585	50.3	1102	0.004496	329.0
586	35.1	1719	0.017359	331.5
587	35.0	1885	0.017871	332.0
588	35.1	1539	0.016651	331.2
589	35.1	1367	0.015603	331.1
590	35.1	1294	0.014871	331.4
591	35.2	1191	0.012254	330.8

Table 3, cont.

Run #	T (°C)	P (psia)	ρ (gmol/cc)	γ (nm)
592	35.3	1170	0.010297	331.2
593	35.2	1134	0.007648	330.7
594	35.2	1123	0.007189	330.6
598	34.8	1798	0.017666	288.1
599	34.8	1704	0.017372	288.1
600	34.9	1530	0.016662	287.6
601	34.9	1370	0.015704	287.3
602	34.9	1287	0.014890	287.3
603	35.0	1201	0.013017	287.1
604	35.1	1173	0.011116	286.8
605	35.0	1130	0.007619	286.2
606	34.9	1103	0.006682	284.0
607	50.5	2058	0.015322	287.3
608	50.1	1914	0.014645	287.6
609	49.9	1694	0.012877	287.3
610	49.9	1543	0.010634	287.3
611	49.9	1374	0.007487	286.8
612	50.0	1288	0.006275	285.2
613	50.0	1203	0.005369	---
614	49.9	1178	0.005148	---
615	49.8	1141	0.004837	---
616	49.9	1102	0.004522	---
617	50.0	2053	0.015412	---
618	49.9	1893	0.014568	---
619	50.0	1721	0.013134	---
620	49.9	1539	0.010560	---
621	50.0	1377	0.007505	---
622	50.0	1274	0.006111	---
623	49.9	1215	0.005496	---
624	50.1	1165	0.005016	---
625	50.2	1150	0.004881	---
626	50.3	1113	0.004579	---
627	49.8	1783	0.011839	329.9
628	49.9	1537	0.010973	330.6
629	49.9	1365	0.010022	329.5
630	49.9	1203	0.008554	329.8
631	49.8	1039	0.006236	330.0
632	49.8	913	0.004568	329.1
633	49.8	860	0.003959	329.1
634	49.8	820	0.003595	328.4

Table 3, cont.

Run #	T (°C)	P (psia)	ρ (gmol/cc)	v (nm)
635	50.0	778	0.003251	328.4
636	50.0	739	0.002964	---
637	50.2	1795	0.011831	331.1
638	50.1	1543	0.010964	329.9
639	50.1	1375	0.010057	330.8
640	50.1	1201	0.008474	329.7
641	50.1	1032	0.006064	329.7
642	50.1	914	0.004489	329.1
643	50.1	862	0.003945	329.1
644	50.0	817	0.003551	328.7
645	50.0	776	0.003229	328.4
646	50.0	741	0.002972	328.6
647	29.6	1794	0.014064	330.4
648	29.9	1546	0.013556	330.3
649	29.9	1371	0.013162	329.8
650	29.9	1202	0.012676	329.9
651	30.0	1032	0.012003	330.1
652	30.0	922	0.011345	330.3
653	30.0	870	0.010858	330.4
654	30.1	808	0.009669	330.0
655	30.1	780	0.008217	329.5
656	30.1	750	0.005612	330.3
657	29.9	1793	0.014029	330.2
658	29.9	1536	0.013534	330.5
659	29.9	1366	0.013145	330.5
660	29.8	1188	0.012654	330.9
661	29.9	1030	0.012017	330.2
662	29.9	912	0.011287	330.3
663	29.9	861	0.010787	330.2
664	30.0	810	0.009806	330.0
665	30.0	779	0.008293	330.2
666	30.0	741	0.005197	329.2
667	29.8	1793	0.014034	285.7
668	29.8	1537	0.013548	285.7
669	29.9	1372	0.013162	285.7
670	30.0	1206	0.012676	285.7
671	29.9	1032	0.012025	285.4
672	29.9	911	0.011207	285.7
673	29.8	872	0.010951	284.9
674	29.9	812	0.009934	285.7
675	29.9	779	0.008452	284.9

Table 3, cont.

Run #	T (°C)	P (psia)	ρ (gmol/cc)	ν (nm)
676	29.9	738	0.005112	285.9
677	49.9	1818	0.011924	285.7
678	49.9	1540	0.010973	285.2
679	49.9	1380	0.010128	284.9
680	49.9	1207	0.008598	284.9
681	49.9	1027	0.006020	---
682	49.9	919	0.004568	---
683	50.1	861	0.003945	---
684	50.1	823	0.003601	---
685	50.1	775	0.003215	---
686	50.1	760	0.003109	---

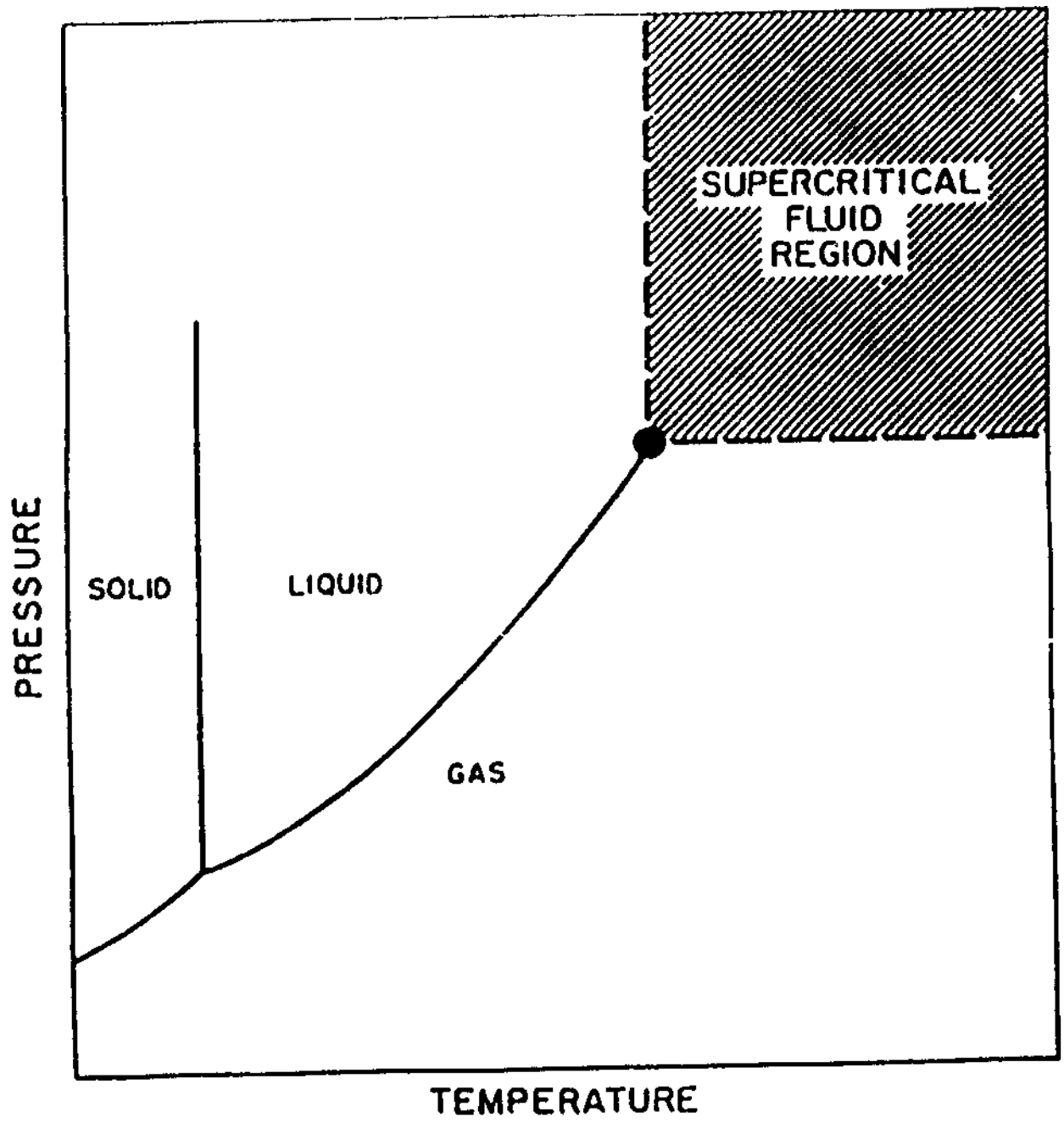

Figure 1 Pressure versus Temperature for a Pure Component

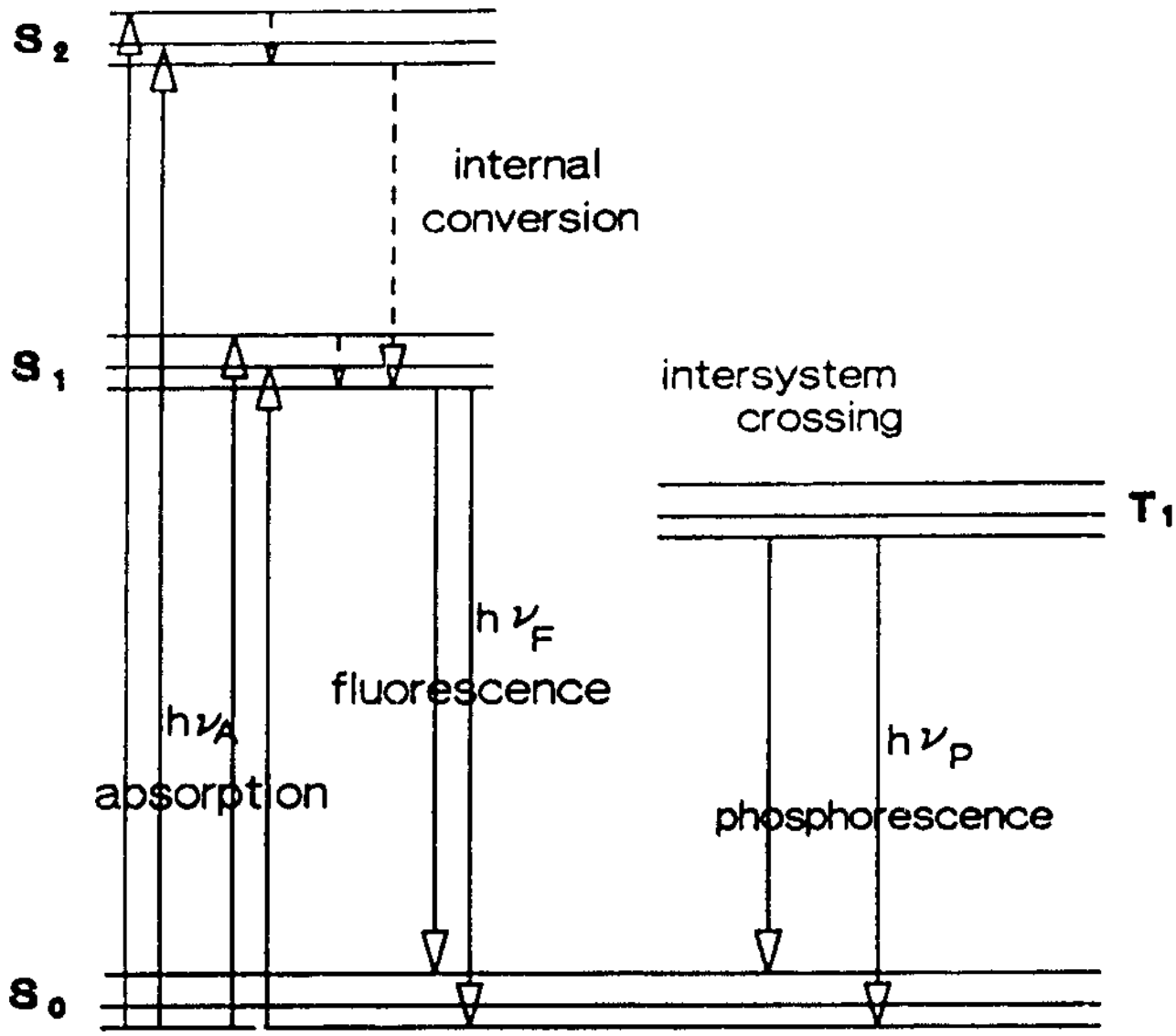

Figure 2 Jablonski Diagram

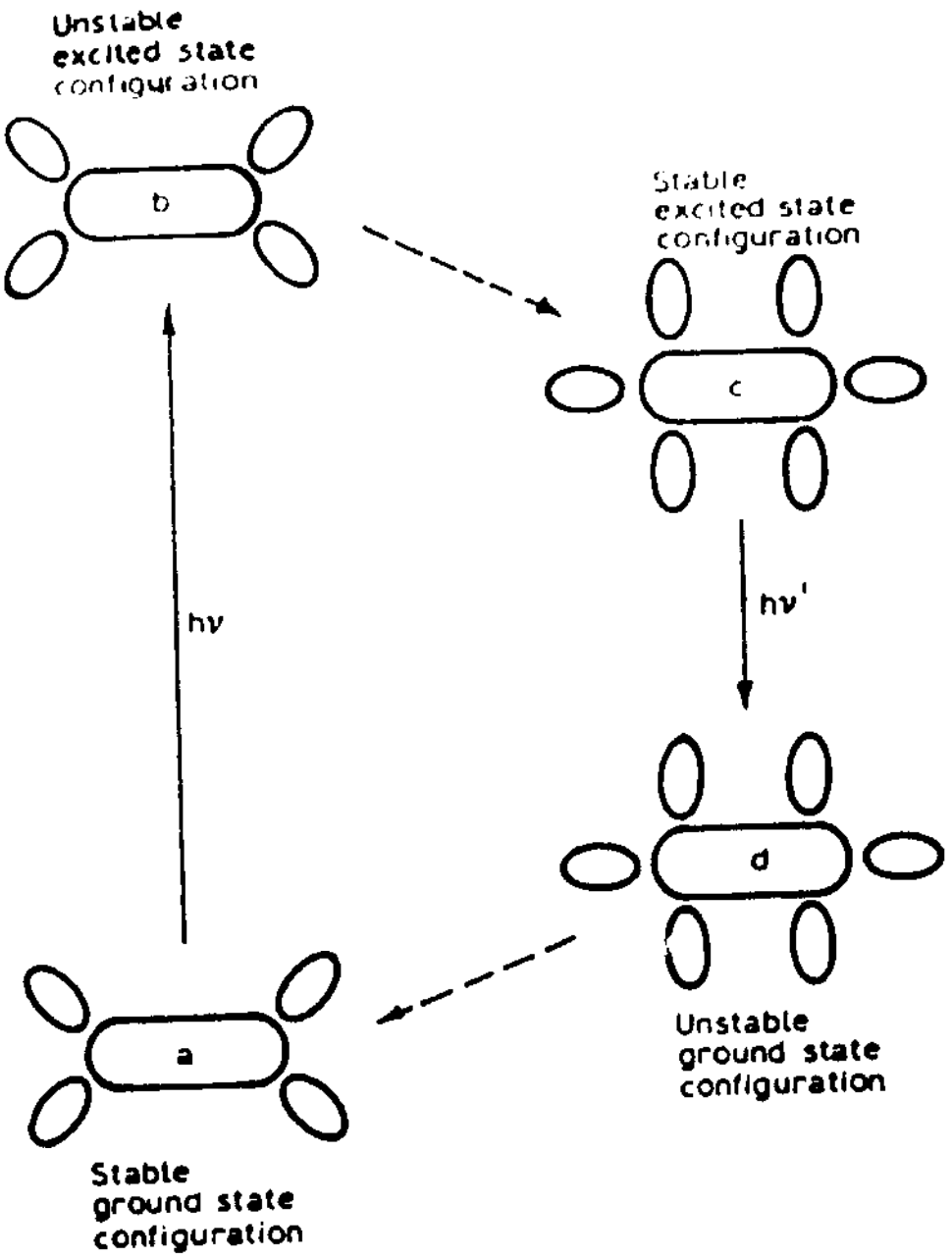

Figure 3 Frequency Shifts by Solvent Rearrangement

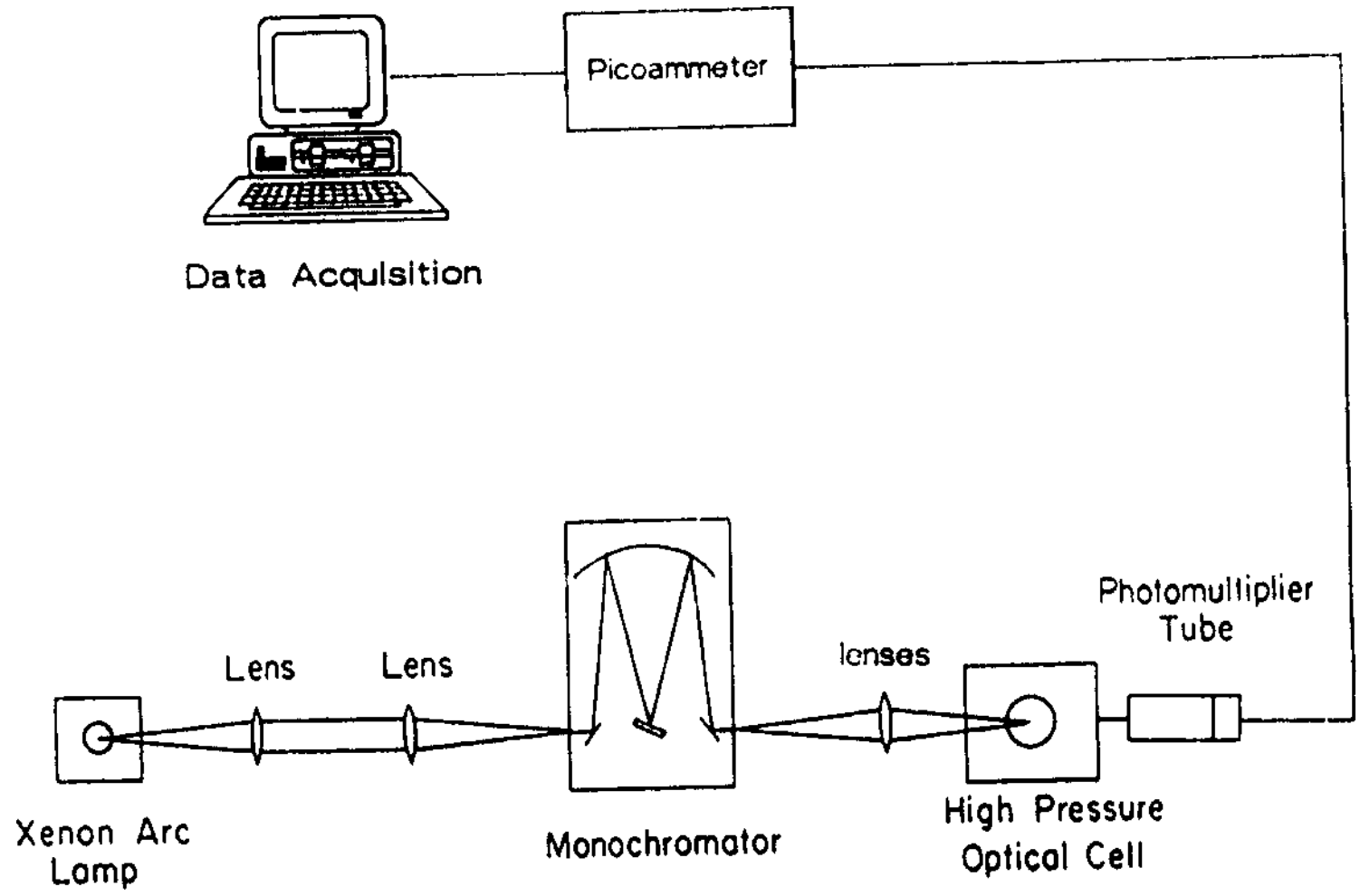

Figure 4a Schematic of Absorption Spectrometer Assembly

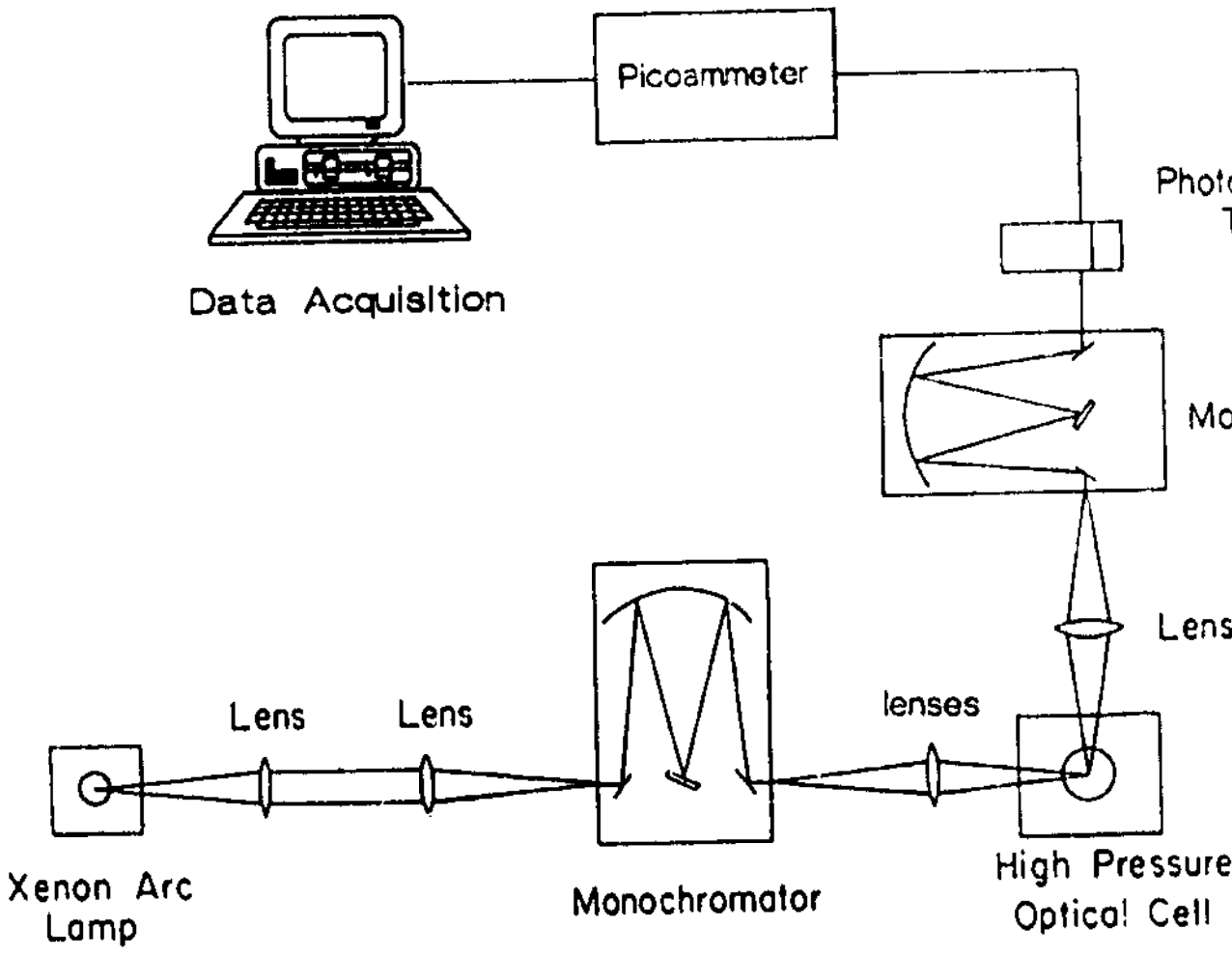

Figure 4b Schematic of Fluorescence Spectrometer Assembly

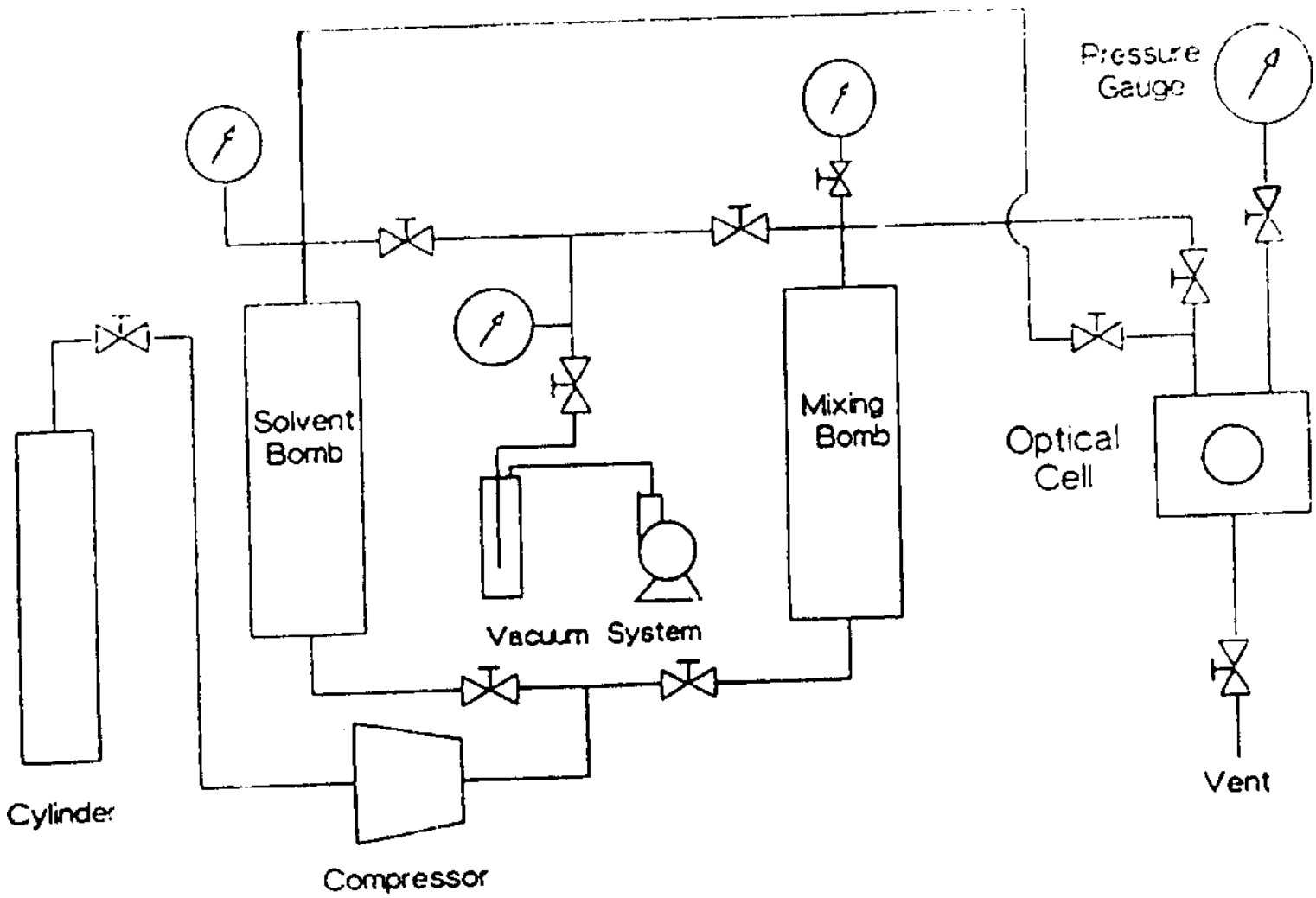

Figure 5 Schematic of High Pressure Assembly

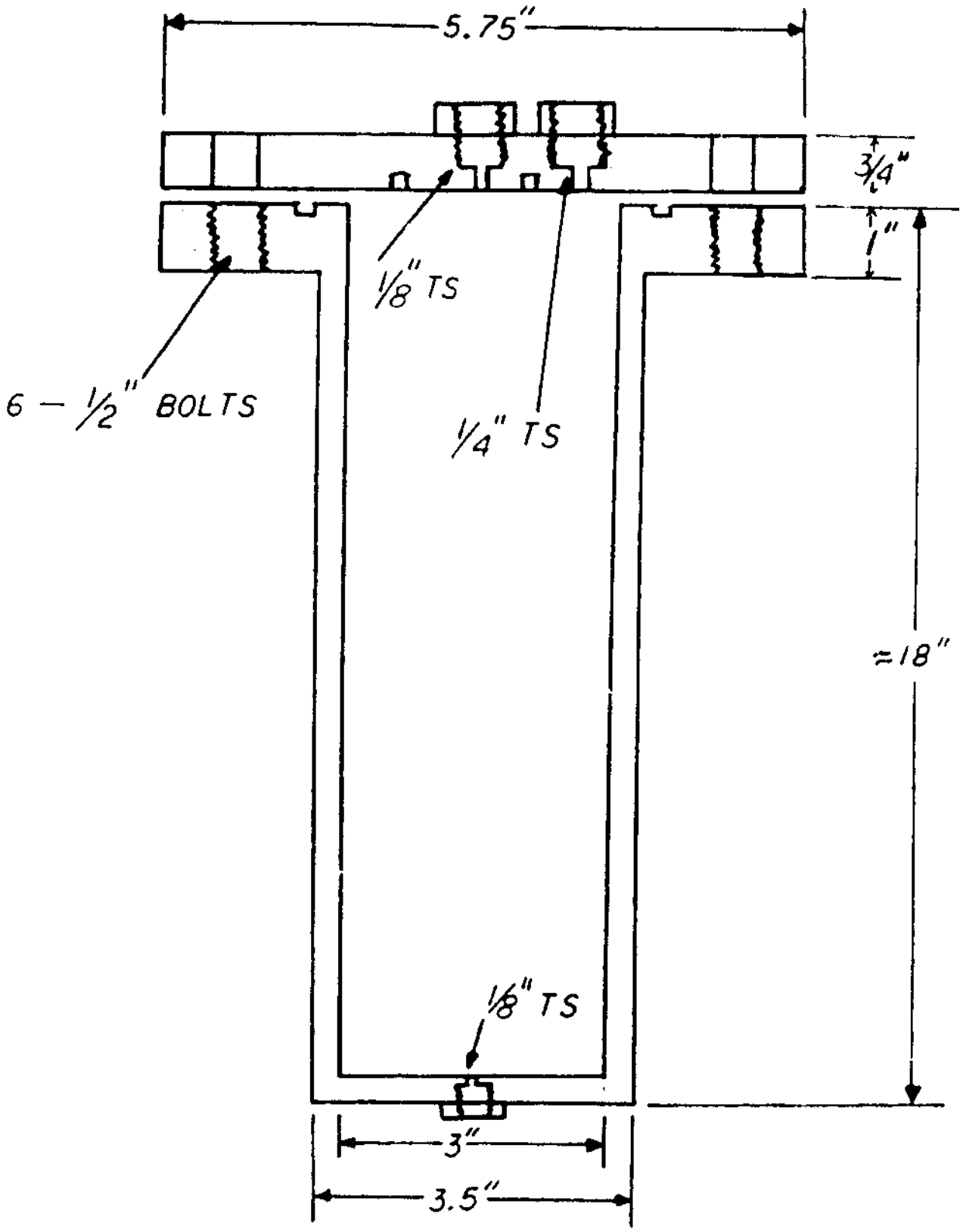

Figure 6 High Pressure Mixing Vessel

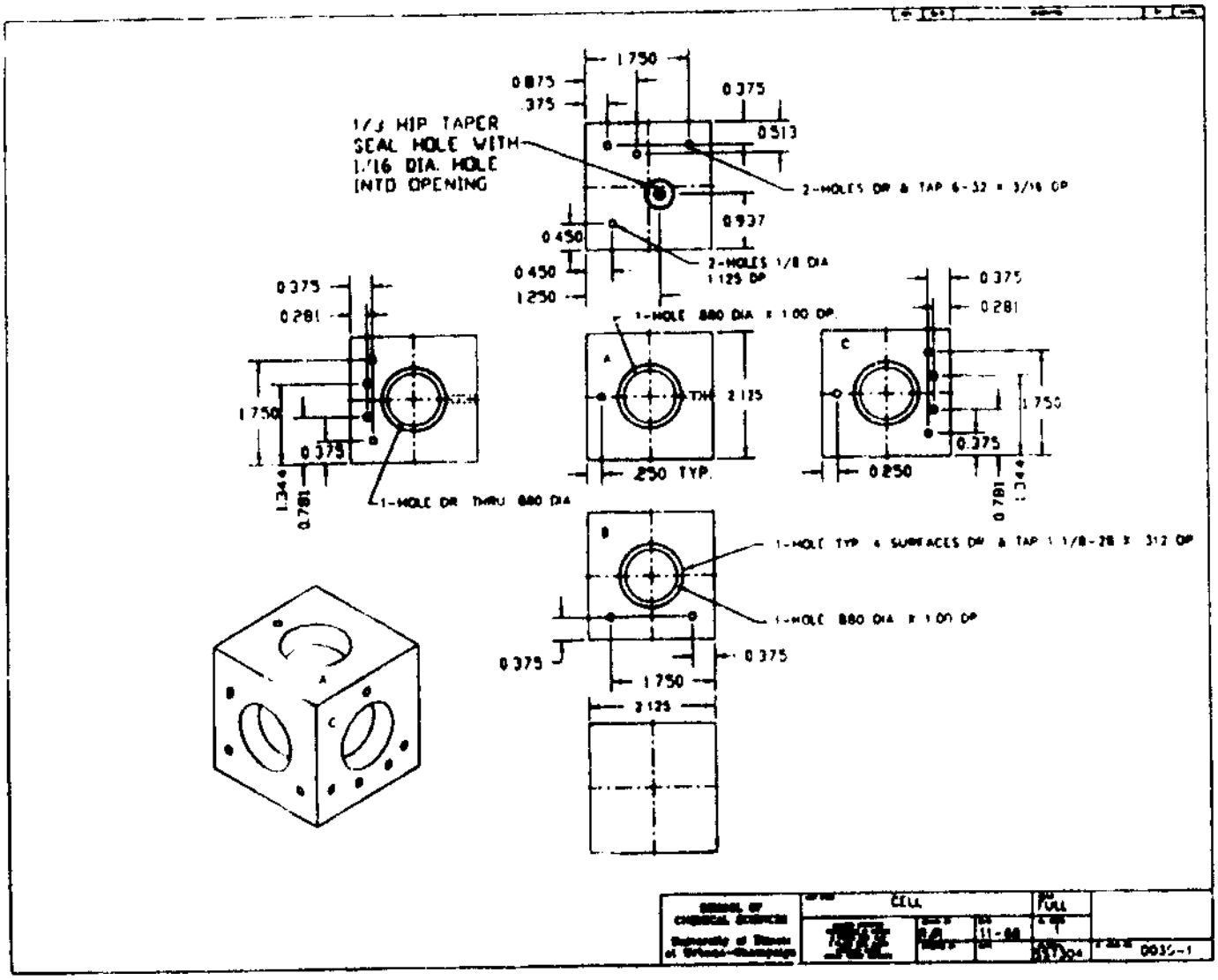

Figure 7 High Pressure Optical Cell

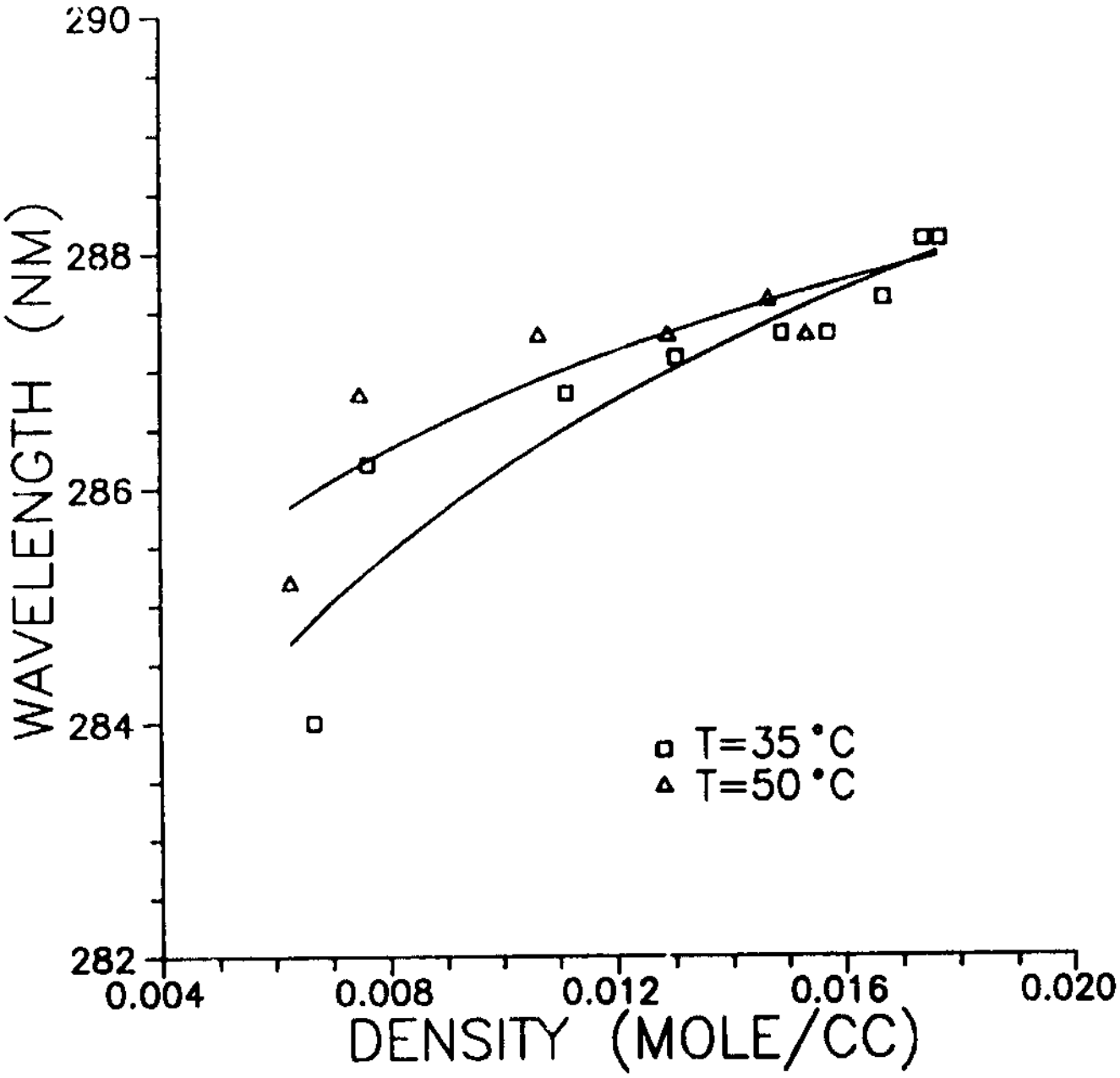

Figure 8 Wavelength versus Density for Absorption Spectra of 10^{-4} Mole Fraction Carbazole in CO_2 at 35 and 50°C

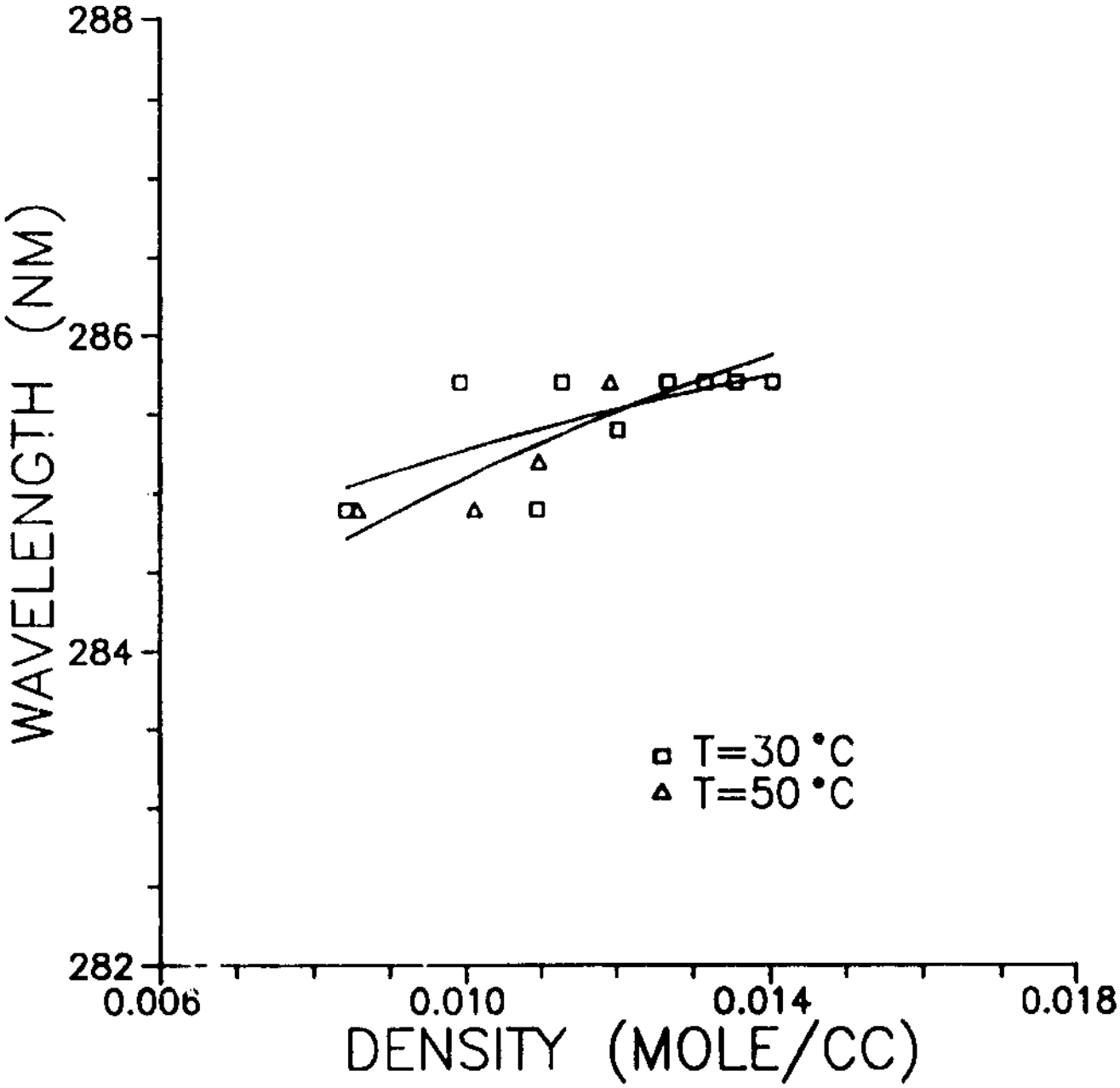

Figure 9 Wavelength versus Density for Absorption Spectra of 10^{-4} Mole Fraction Carbazole in CHF_3 at 30 and 50°C

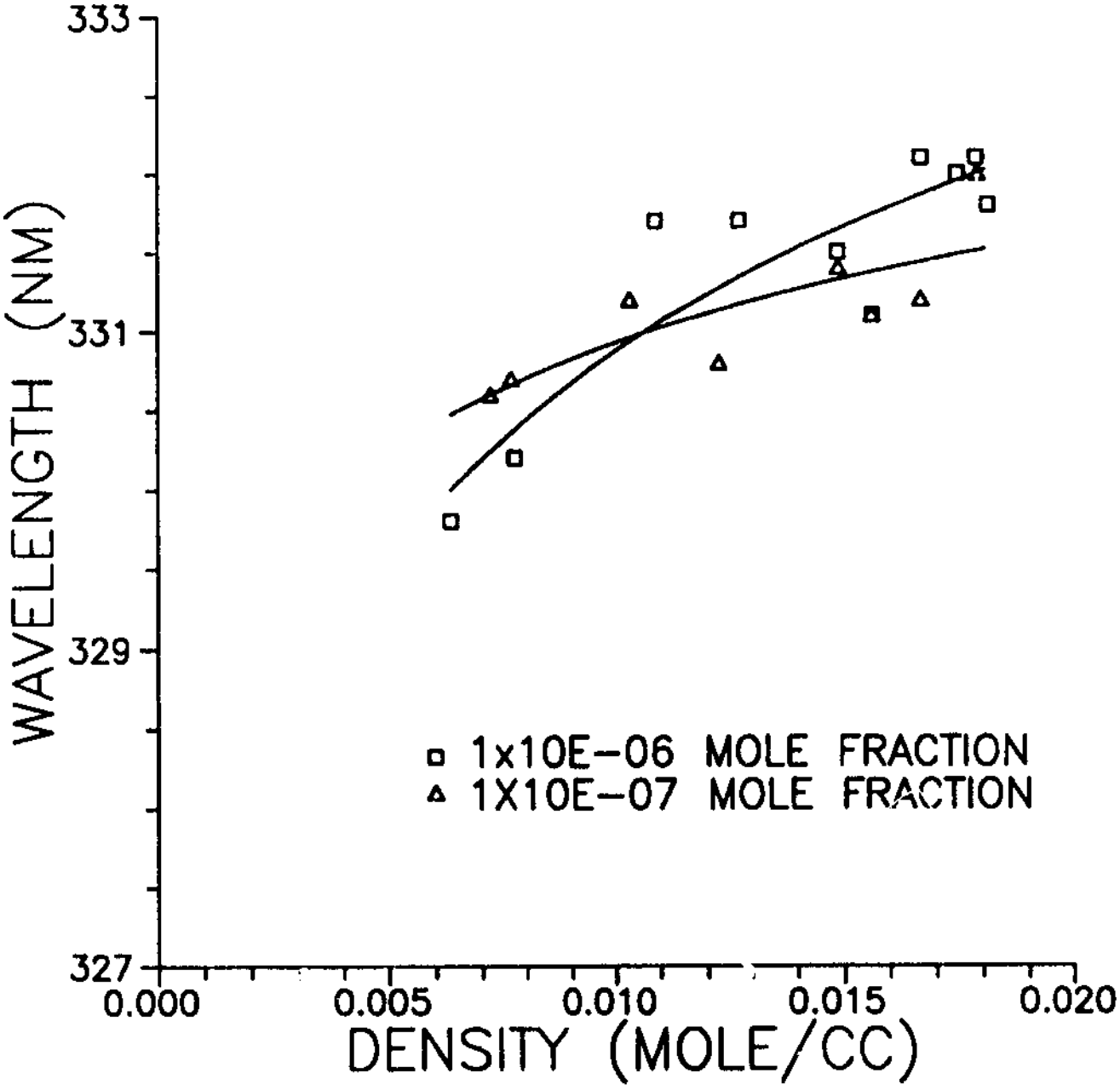

Figure 10 **Wavelength versus Density for Absorption Spectra of 10^{-6} and 10^{-7} Mole Fraction Carbazole in CO_2 at 35°C**

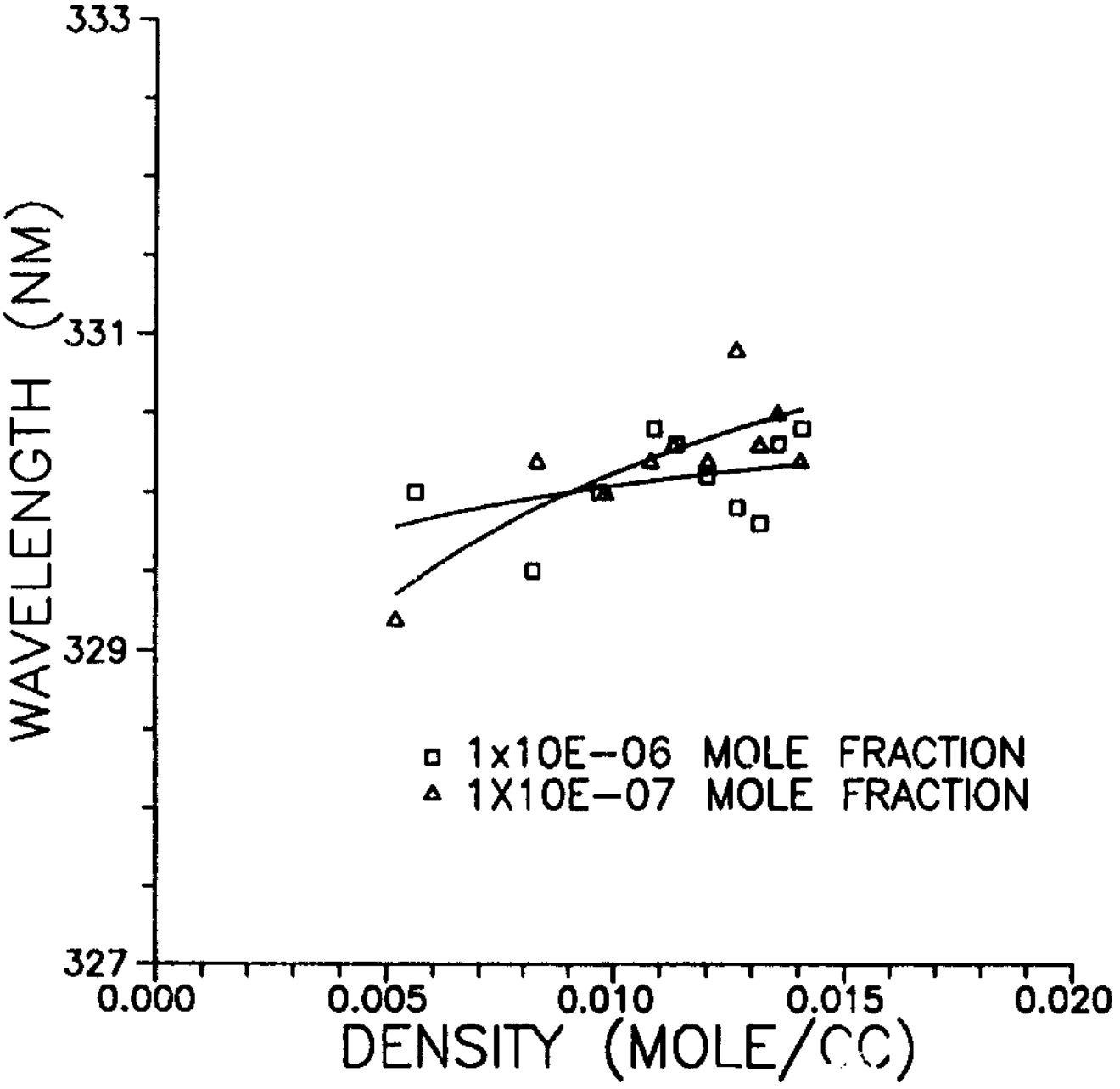

Figure 11 Wavelength versus Density for Fluorescence Spectra of 10^{-6} and 10^{-7} Mole Fraction Carbazole in CHF_3 at 30°C

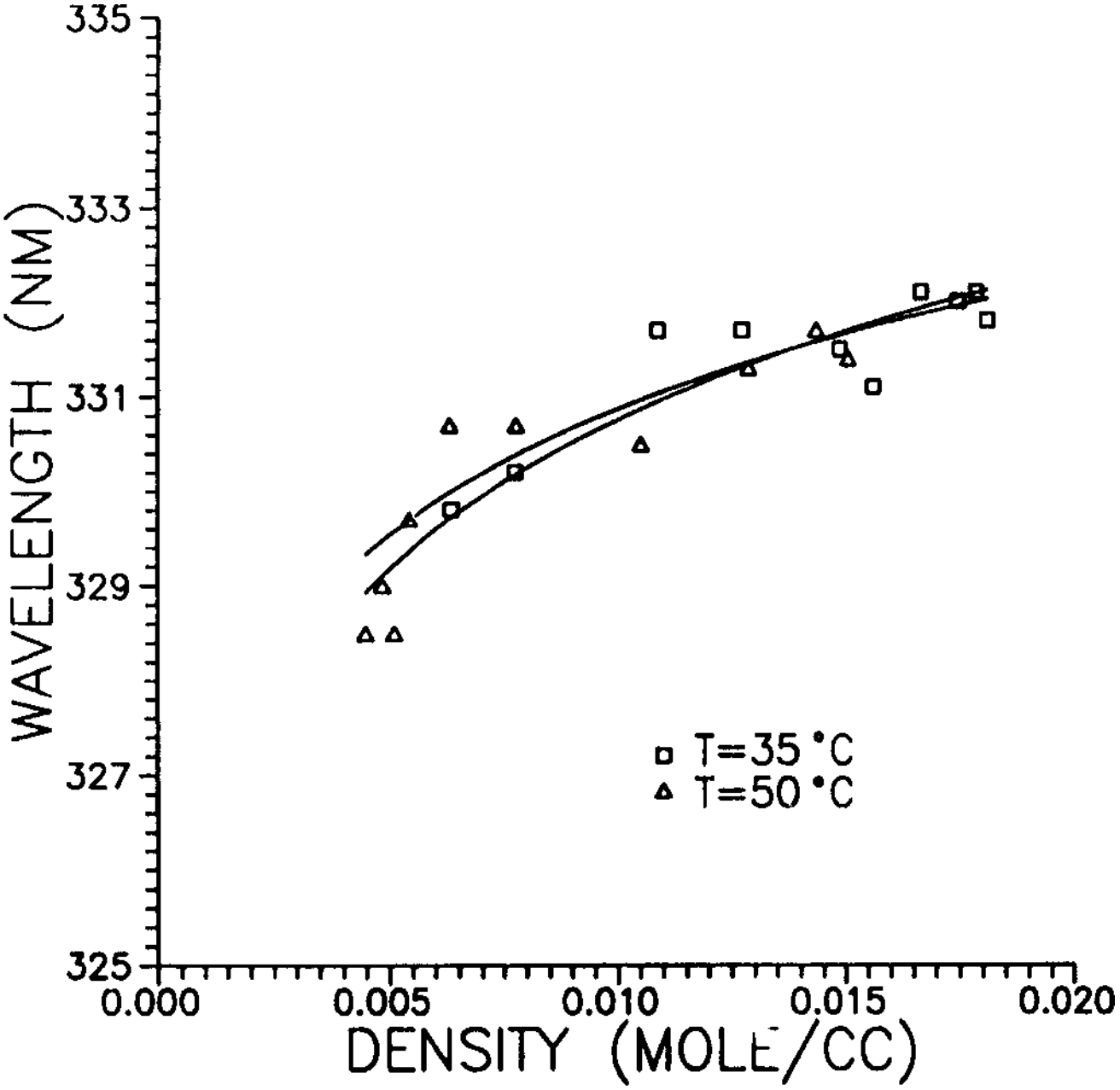

Figure 12 Wavelength versus Density for Fluorescenece Spectra of 10^{-4} Mole Fraction Carbazole in CO_2 at 35 and 50°C

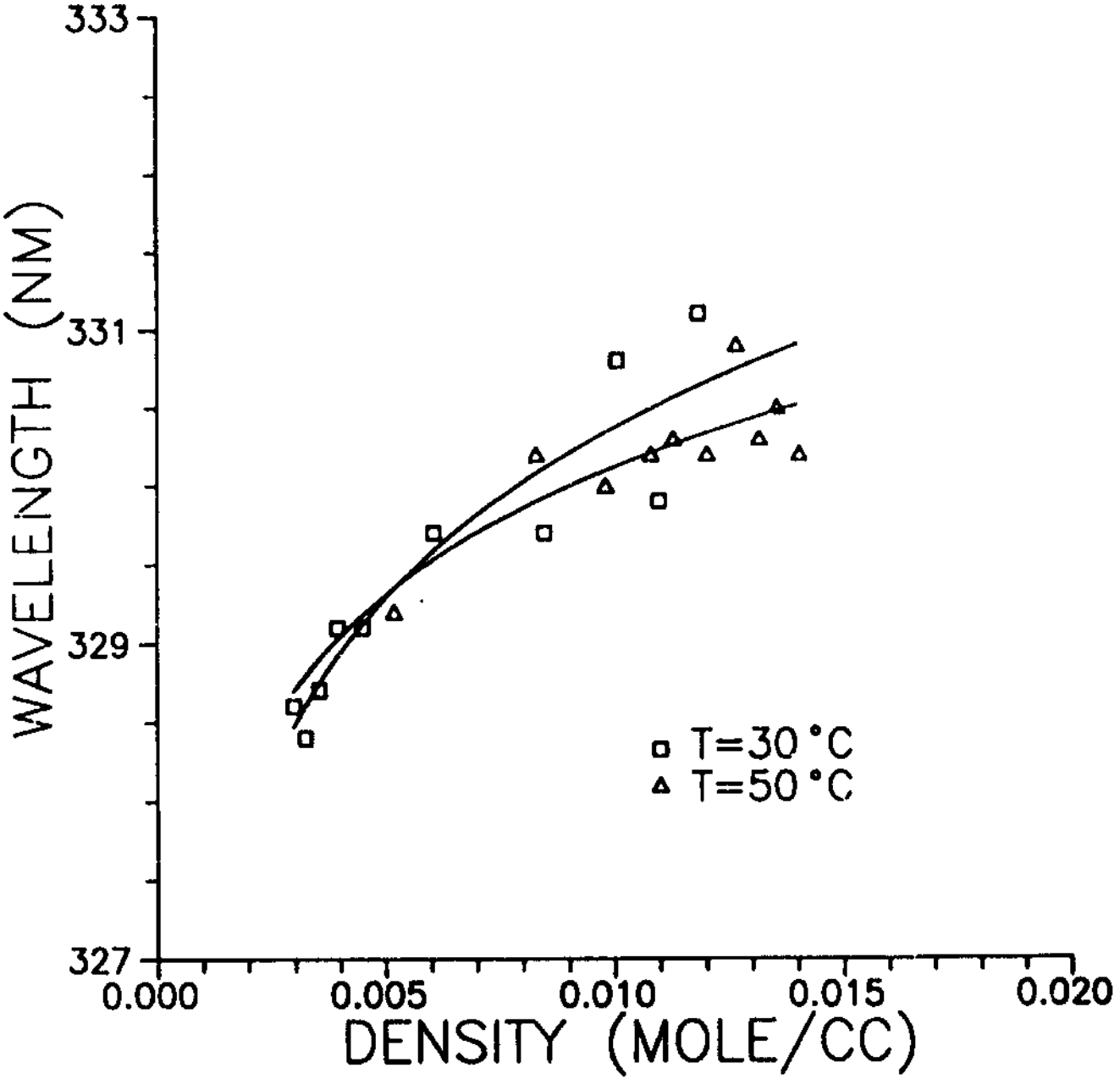

Figure 13 Wavelength versus Density for Fluorescenece Spectra of 10^{-4} Mole Fraction Carbazole in CHF, at 30 and 50°C

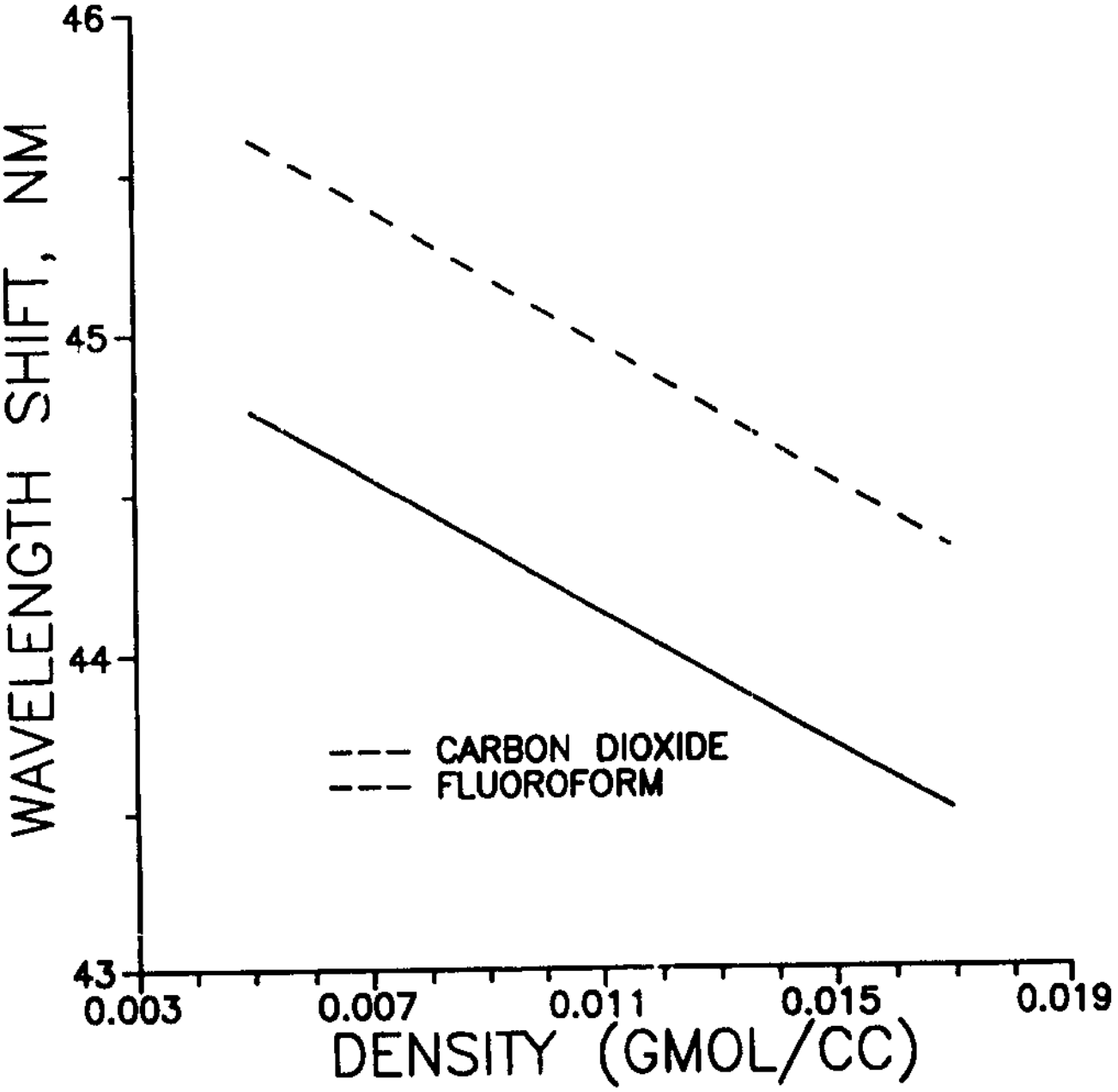

Figure 14 Wavelength Shift ($\nu_s - \nu_f$) versus Density for Carbazole in CO_2 and CHF_3